doi:10.22364/mmp2017.27

VIII International Scientific Colloquium
Modelling for Materials Processing
Riga, September 21 - 22, 2017

Comparison of Single and Consecutive Dual Frequency Induction Surface Hardening of Gear Wheels

J. Barglik, K. Ducki, D. Kukla, J. Mizera, G. Mrówka-Nowotnik, J. Sieniawski, A. Smalcerz

Abstract

Mathematical modeling of single and consecutive dual - frequency induction surface hardening systems are presented and compared. The both models are solved by the 3D FEM-based professional software supported by a number of own numerical procedures. The methodology is illustrated with some examples of surface induction hardening of a gear wheel made of steel 41Cr4. The computations are in a good accordance with experiments provided on the laboratory stand.

Introduction

Induction hardening is a kind of heat treatment where a steel body or its selected part is heated by induction to an appropriate temperature and then immediately quenched. Its result is very hard, but brittle microstructure. The idea of the surface induction hardening is connected with hardening of a thin surface layer only and keeping soft the internal part of the treated material. In general, the induction surface hardening consists of two consecutive stages with a short austenitization break between them. The time evolution of the process are presented in Fig.1 for the single frequency induction hardening (SFIH) and in Fig. 2 for the consecutive dual frequency induction hardening (CDFIH)

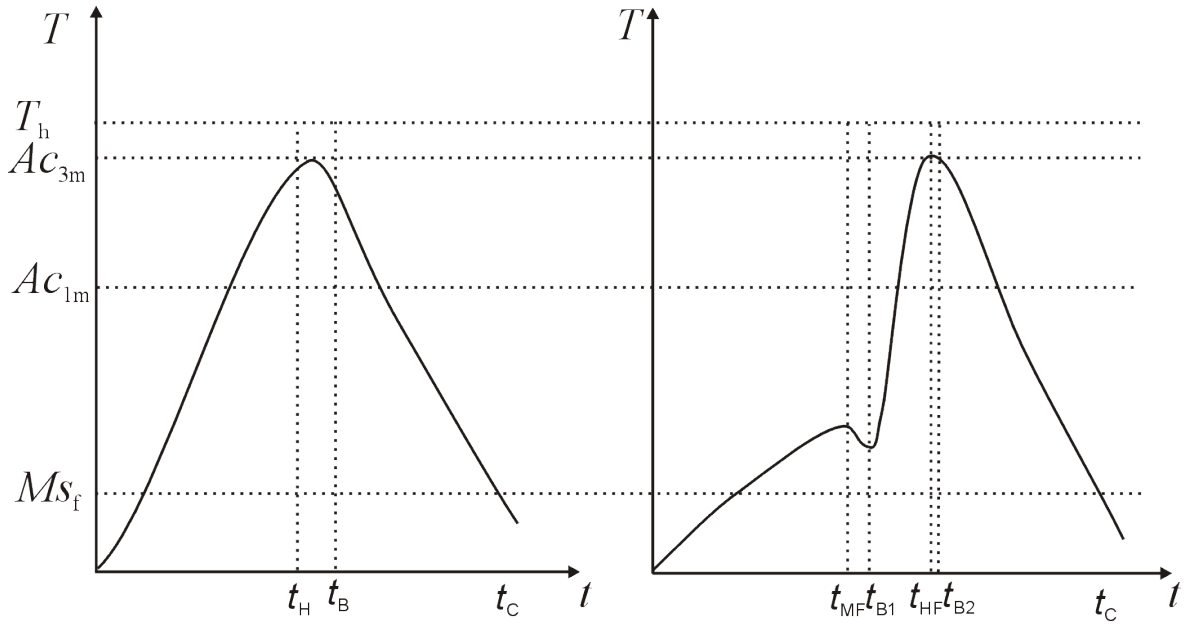

Fig.1 Time evolution of temperature during single (on left) and dual frequency induction surface hardening (on right)

The first stage of the SFIH process is the fast induction heating. In a thin surface layer the treated material reaches the hardening temperature T_h being bigger than the modified upper critical temperature Ac_{3m} at [1].

$$T_h = T\big|_{t=t_B} \geq Ac_{3m} \tag{1}$$

where t_B denotes the time when cooling begins (see Fig.1).

For deeper layers the hardened body reaches temperatures bigger than the modified lower critical temperature Ac_{1m}, but smaller than the modified upper critical temperature Ac_{3m} and the microstructure contains not only austenite, but also pearlite and carbides.

$$A_{c3m} \geq T\big|_{t=t_B} \geq A_{c1m} \tag{2}$$

Finally, for the internal part of the body the material does not contain austenite at all.

$$T\big|_{t=t_B} \leq A_{c1m} \tag{3}$$

For the dual-frequency process, the induction heating could be realized as simultaneous or consecutive. In the latter case the heating is realized in two consecutive time steps Δt_{MF} and t_{HF} with a short break between them Δt_{B1}. The first step is the medium frequency (MF) induction heating. Then almost immediately (short break time t_{B2}) the high frequency (HF) induction heating is realized. The heating terminates when the average temperature in the hardened zone exceeds Ac_{3m}. However it depends on velocity of heating. In order to determine it the Time-Temperature-Austenitization (TTA) diagram for the steel is measured (Fig. 2).

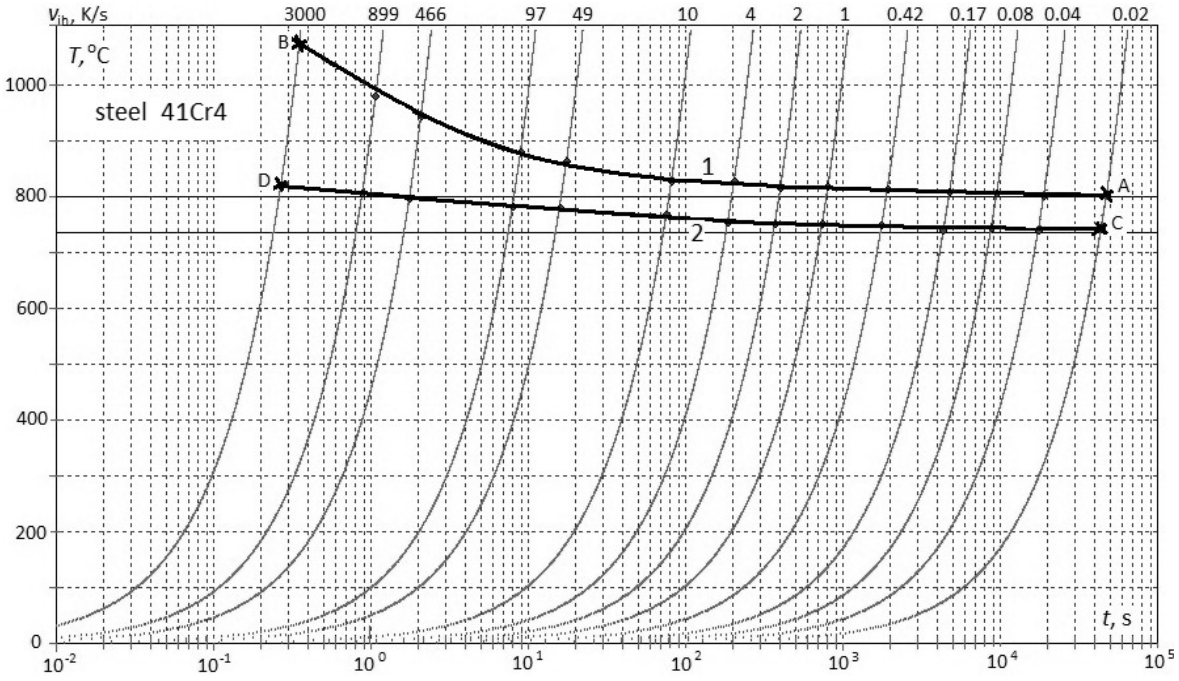

Fig. 2. TTA diagram for steel 41Cr4

Curve 1 in Fig. 2 represents dependence of Ac_{3m} on velocity of induction heating v_{ih}. For slow heating $Ac_3 = 801^0$C (point A at the curve 1). For very fast heating the modified upper criterial temperature Ac_{3m} is distinctly bigger. For velocity of heating $v_{ih} = 3000$ K/s $Ac_{3m} = 1075^0$C (point B at the curve 1). Curve 2 in Fig. 2 represents dependence of Ac_{1m} on velocity of induction heating v_{ih}. For slow heating $Ac_1 = 736^0$C (point C at the curve 2). For very fast

heating the modified lower criterial temperature Ac_{1m} is bigger. For v_{ih} = 3000 K/s Ac_{1m} = 805^0C (point D at the curve 2). The second stage – quenching – makes it possible to achieve the requested martensitic microstructure. The resultant hardness depends on the speed of cooling. The real character of this dependence can be determined from the Continuous Cooling Temperature (CCT) diagram. For steel 41Cr4 in order to obtain uniform martentisic microstructure the velocity of cooling should be bigger than 500 K/s and the final temperature lower than the martensite finish temperature Ms_f. During a short break between both stages the temperature of the body decreases, but for the surface layer ii is still higher than Ac_{3m}.

1. Mathematical modelling

In the paper we focus our attention on the spin induction hardening, where the material is heated simultaneously by a suitable inductor. We use single and dual-frequency hardening systems which allows obtaining the prescribed hardness profile. From the physical viewpoint, induction heating is a strongly nonlinear multi-physic process (Fig. 3). The interaction between fields are connected mostly with temperature dependences of material properties. Electromagnetic and temperature fields were analyzed by means of FEM-based software. The total volumetric power density p_v consists of two components, but the hysteresis losses are neglected:

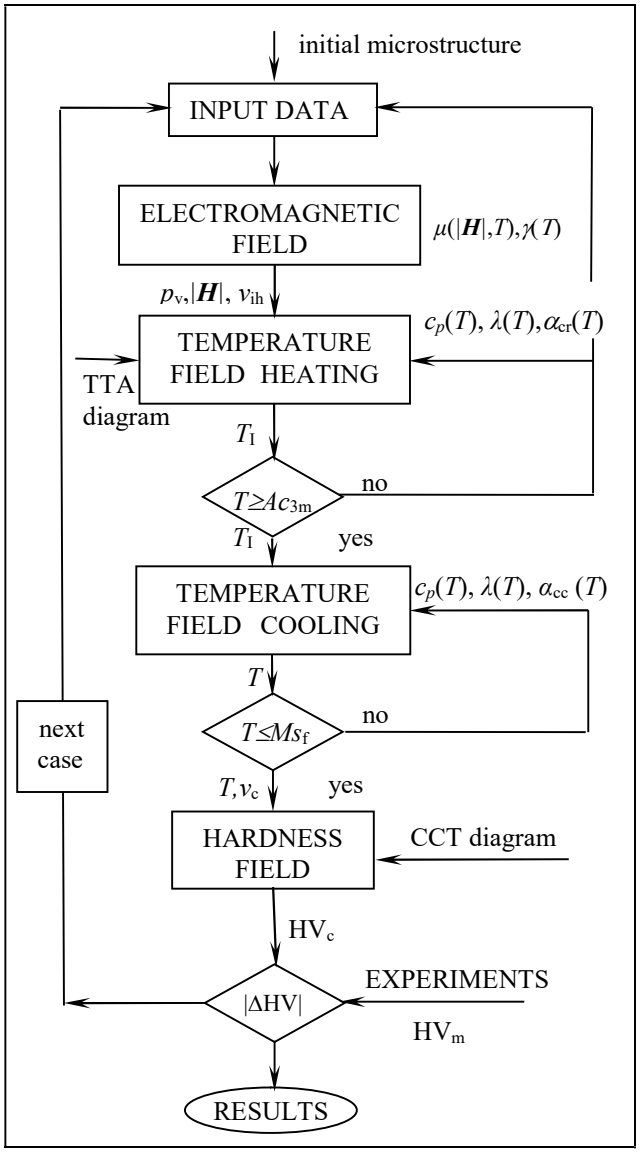

Fig. 3. Algorithm of the computation

$$p_v = p_H + p_J \tag{4}$$

$$p_H = p_H\left(|\boldsymbol{H}|, f\right) \tag{5}$$

$$p_v \approx p_J = \frac{|\boldsymbol{J}_{ind}|^2}{\gamma}, \tag{6}$$

where $\boldsymbol{H}$ denotes the magnetic strength, f the frequency, $\boldsymbol{J}_{ind}$ eddy current density and γ electric conductivity.

Dependences of the specific heat c_p, the thermal conductivity λ, and the electric conductivity γ on temperature are shown in Fig. 4 – 6. Dependence (7) of the relative magnetic permeability μ_r on temperature for $|\boldsymbol{H}| = \text{const}$ was shown in Fig. 7 [2].

$$\mu_r = f(|\boldsymbol{H}|, T). \tag{7}$$

The heat transfer was given by (8)

$$-\lambda \cdot \frac{\partial T}{\partial n} = \alpha_c\left(T - T_{ac}\right) + \sigma_o \varepsilon\left(T^4 - T_{ar}^4\right), \tag{8}$$

where α_c denotes convection heat transfer coefficient, T_{ac} temperature of convection environment, σ_0 – Stefan constant, ε – emissivity, T_{ar} – temperature of radiation environment.

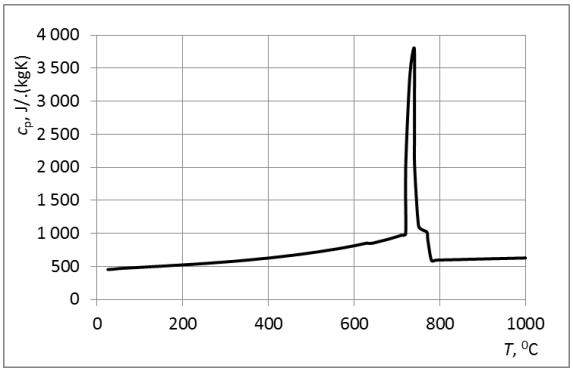

Fig. 4. Dependence of the specific heat on temperature

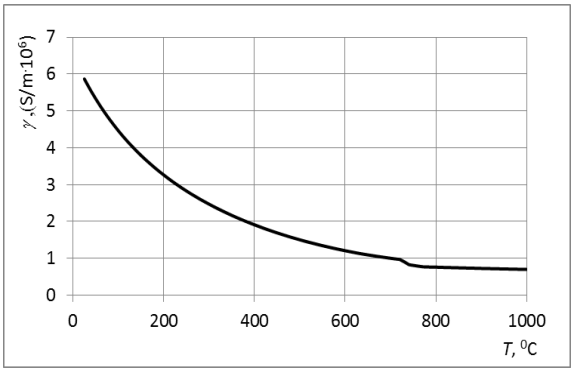

Fig. 5. Dependence of the electric conductivity of temperature

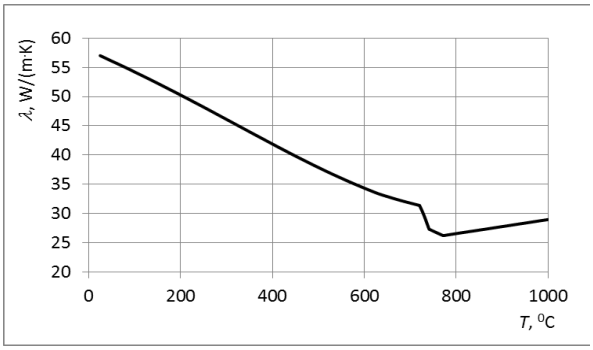

Fig. 6. Dependence of thermal conductivity on temperature

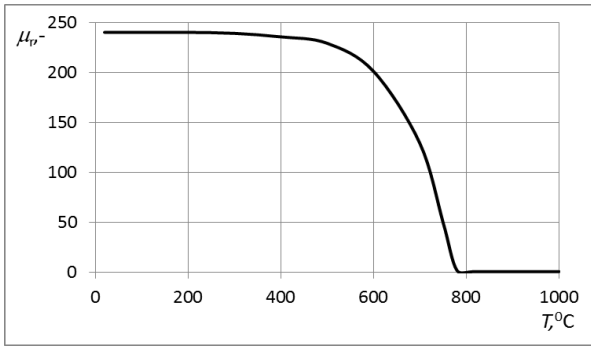

Fig. 7. Dependence of the relative magnetic permeability on temperature

The computation of temperature field for induction heating terminates when the average temperature of the hardening zone exceeds Ac_{3m}. Then temperature field for cooling by spraying was calculated. Dependences of the specific heat c_p, the thermal conductivity λ and convection heat transfer α_{cc} on temperature were taken into account. The computation of temperature field for cooling terminates when the inequality (9) was satisfied.

$$T\big|_{t=t_C} \le Ms_f \tag{9}$$

where t_C denotes the time when cooling terminates and Ms_f means the temperature when the martensite transformation is completed.

And finally hardeness and microstructure distribution were determined and compared with measurements.

2. Illustrative Example

The numerical solution of the induction hardening of gear wheels was provided by the Flux3D software with some own procedures. An attention was paid to the convergence of results in the dependence on the density of discretization meshes for the electromagnetic and temperature fields and on the position of the artificial boundary ABCD (Fig.1).

Basic parameters and dimensions of the system are as follows:

Gear wheel: teeth number n = 16, width of the tooth ring b = 0.006 m, external diameter d_c = 0.0356 m, internal diameter d_i = 0.0269 m, diameter of the hole d_h = 0.016 m, material: steel 41Cr4 (its chemical composition is presented in Tab. 1):

Tab. 1. Chemical composition of steel 41Cr4

Element	C	Cr	Si	Mn	Ni	Cu	P
%	0.4	1.05	0.24	0.73	0.16	0.16	0.025

MF inductor (upper part of Fig. 8): number of coils - 1, external diameter 0.054 m, internal diameter 0.0395 m, height 0.007 m, length of busbars 0.363 m, distance between them 0.003 m

HF inductor (lower part of Fig. 8): number of coils – 1, external diameter 0.061 m, internal diameter 0.0395 m, height of coil 0.007 m total height (coil + concentrator) 0.021 m, flux concentrator: its external diameter 0.0815 m, its internal diameter 0.039 m, thickness of 2x0.005 m.

Sprayer : distance between inductor and sprayer 0.02 m, external diameter 0.085 m, internal diameter 0.061 m, quenchant: polymer solution.

Heat transfer parameters: radiation for heating only, the temperature of convection and radiation environment $T_{ac} = T_{ar} = 20^0$C, the heat transfer coefficient during heating $\alpha_{cr} = 20$ W/(m^2·K), temperature of quenchant $T_q = 30^0$C, convection heat transfer coefficient during cooling $\alpha_{cc} = 1200$ W/(m^2·K),

Modified criterial temperatures for real heating conditions: heating velocity $v_h = 200 – 400$ K/s, $Ac_{3m} = 920^0$C, $Ac_{1m} = 720^0$C, hardening temperature $T_h = 970^0$C,

Fig. 8. MF inductor (up) and HF inductor – sprayer (down)

Parameters of the induction heating for various cases: medium frequency: power of the generator: $P_{MF} = 60$ kW, current $I_{MF} = 1385$ A, heating time $\Delta t_{MF} = 4 – 6$ s, frequency $f = 36$ kHz, high frequency: $P_{HF} = 20$ kW, current $I_{HF} = 500$ A, frequency $f = 280$ kHz, $\Delta t_{HF} = 0.6 – 0.8$ s, rotation velocity $v_r = 2$ r/s.

Breaks: between heating and cooling: $\Delta t_B = 0.2$ s, between MF and HF heating $\Delta t_{B1} = 0.5$ s.

Below three examples of the induction hardening were presented. First the CDFIH process was analyzed for following parameters: MF heating: $t_{MF} = 4$ s, $I_{MF} = 1385$ A, $f_{MF} = 36$ kHz, Break: $\Delta t_{B1} = 0.5$s, HF heating: $\Delta t_{HF} = 0.7$s, $I_{HF} = 500$A, $f_{HF} = 240$ kHz.

Temperature distribution within the tooth after MF heating is presented on left part of Fig. 9. For $\Delta t_{MF} = 4$ s average temperature within the tooth $T_{av1} = 475^0$C, which is sufficiently lower than Ac_{1m}. After HF heating the average temperature in the thin hardened zone along the working surface of the tooth $T_{av2} = 923^0$C.

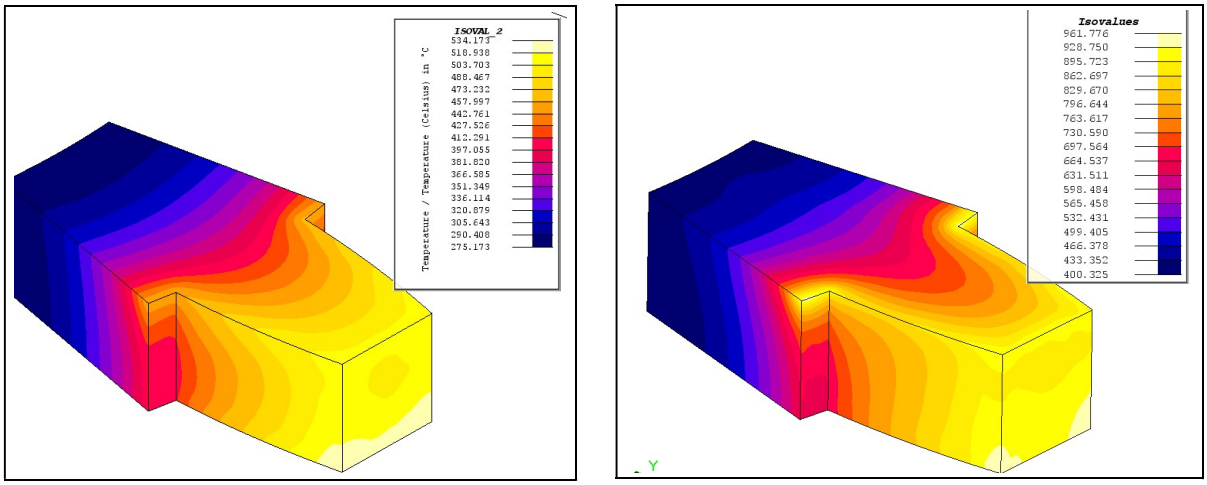

Fig. 9. CDFIH process. Temperature distribution: MF heating (left) and HF heating (right)

And the second and the third case the SFIH process were analyzed for the same current and frequency ($I_{MF} = 1385$ A, $f_{MF} = 36$ kHz; $I_{HF} = 500$ A, $f_{HF} = 240$ kHz) and for the longer time of heating $t_{MF} = 6.6$ s, $t_{HF} = 1.5$ s. Temperature distribution after SFIH heating was presented in left side (MF) and right side of Fig. 10.

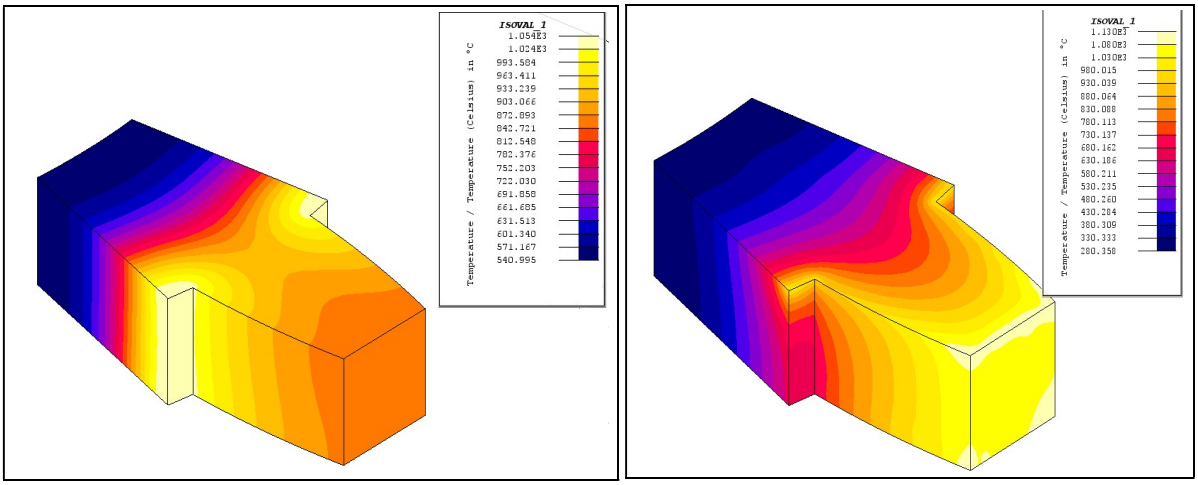

Fig. 10. SFIH process. Temperature distribution MF heating (left) and HF heating (right)

For t_{MF} = 6.6 s the average temperature within the tooth T_{av} = 935^{0}C. Taking into account calculated velocity of heating v_{ih} = 140 K/s the final temperature was sufficiently higher than Ac_{3m}. But it was characteristic the non-uniform temperature distribution. At the top of the tooth the average temperature T_{avtop} = 820^{0}C only. For t_{HF} = 1.5 s the average temperature in the thin hardened zone along the working surface of the tooth T_{av} = 953^{0}C. Taking into account that for the case calculated velocity of heating v_{ih} = 620 K/s the final temperature was still higher than Ac_{3m}. The temperature distribution in the hardened zone was more uniform in comparision with the previous case. Based upon results (Fig. 9 – 10) hardness distribution was calculated. Computations were compared with the measurements and quite reasonable accordance between them was noticed. Details will be presented during the conference.

3. Summary

The paper presents the SFIH and CDFIH methods applied for induction hardening of small gear wheels made of steel 41Cr4. Computations were compared with measurements of hardness distribution and the reasonable accuracy was achieved, however for the expected contour hardness distribution was obtained for the CDFIH method only.

Acknowledgment

The paper was granted by the National Center for Research and Development under project PBS2/A5/41/2014.

References

[1] Barglik J.: Mathematical modeling of induction surface hardening, 2016, „Compel-the international journal for computation in mathematics in electrical and electronic engineering", Vol. 35, Issue 35, pp. 1403 – 1417.

[2] Barglik J., Smalcerz A.: Influence of the magnetic permeability on modeling of induction surface hardening, 2017, „Compel-the international journal for computation in mathematics in electrical and electronic engineering", Vol. 36, Issue. 2, pp. 555 – 564.

Authors

Prof. Barglik, Jerzy
Dr hab. Ducki, Kazimierz
Dr hab. Smalcerz, Albert
Silesian University of Technology
ul. Krasińskiego 8
40-019 Katowice, Poland
jerzy.barglik@polsl.pl

Dr Kukla, Dominik
Prof. Mizera, Jarosław
Warsaw University of Technology
ul. Wołoska 141
02-507 Warszawa, Poland
jmizera@inmat. pw. edu.pl

Dr hab. Mrówka-Nowotnik, Grażyna
Prof. Sieniawski, Jan
Rzeszów Technical University
ul. Żwirki i Wigury 4
35-959 Rzeszów, Poland
jansien@prz.edu.pl